

WHEN PHOTOIONIZATION IS NOT ENOUGH

Sueli M. Viegas

Instituto Astronômico e Geofísico, USP, Brazil

RESUMEN

Es bien sabido que la fotoionización es el mecanismo principal que produce las líneas de emisión en nebulosas. Durante cerca de 30 años, se han empleado simulaciones numéricas basadas en códigos de fotoionización para analizar regiones H II, nebulosas planetarias y núcleos de galaxias activas. Aunque estos modelos pueden reproducir muchos de los detalles observados, hay algunos que permanecen inexplicados. Dos causas posibles para estas discrepancias entre las observaciones y las predicciones de los modelos se discuten en este artículo: (a) los modelos no son suficientemente realistas; (b) se necesita una fuente de energía adicional. La discusión aquí está principalmente basada en los resultados de los modelos de fotoionización para el nudo NO de I Zw 18.

ABSTRACT

It is well-known that photoionization is the major mechanism powering nebulae emission-lines. For about 30 years, numerical simulations using photoionization codes have been employed to analyze H II regions, planetary nebulae and active galactic nuclei. Although these models can reproduce most of the observed features, some remain unexplained. Two possible causes for the discrepancies between observations and model predictions are discussed in this paper: (a) the models are not realistic enough; (b) an additional energy source is needed. The discussion here is mainly based on the results of photoionization models for the NW knot of I Zw 18.

Key Words: **GALAXIES: ACTIVE — GALAXIES: INDIVIDUAL (I ZW 18) — H II REGIONS — SHOCK WAVES**

1. INTRODUCTION

The emission-line spectra of planetary nebulae, H II regions and active galactic nuclei have been largely used to derive the physical conditions and elemental abundances in these objects. An empirical method proposed by Peimbert & Costero (1969) is usually used, providing average values of the electron temperature and density of the emitting gas, as well as of the ionic fractions and elemental abundances, from the observed emission-line intensities. Since the main mechanism powering the emitting regions is photoionization, numerical simulations based on photoionization codes have also been used to study those objects.

Since the 1960's, photoionization codes have been developed and became a powerful tool to analyze the emission-line spectra of those objects. Presently, several such codes are available (see, for instance, Ferland et al. 1995), one of the most popular being Cloudy (Ferland 2000). Until recently, only these one-dimensional (1-D) codes, assuming spherical or plane-parallel symmetry, were available. In the last few years, some effort has been devoted to develop 3-D simulations (Gruenwald, Viegas & Brogière 1997; Och, Lucy & Rosa 1998).

The 1-D photoionization codes have been used either to derive the general properties of a given class of emission-line objects or to obtain a detailed analysis of selected objects. In the first case, a grid of models is used to create diagnostic diagrams where theoretical and observational data are compared. On the other hand, detailed analysis of a given object, with observations available in a large wavelength range, provides a test for the physical processes occurring in the gas. However, even for H II regions and planetary nebulae, which are surely powered by photoionization, the usual 1-D models fail to reproduce all their properties. The main problems are:

- (a) The observed radio brightness temperature is lower than predicted by the models. To overcome this problem, it is usual to include a filling factor in the calculations, as proposed by Osterbrock & Flather (1959).
- (b) The discrepancy between the temperatures derived from the [O III] lines and from the Balmer lines is not explained by the models (see, for instance, Liu & Danziger 1993). The discrepancy may be solved if the codes include either condensations (Viegas & Clegg 1994) or

additional heating to produce temperature fluctuations (Mathis, Torres-Peimbert & Peimbert 1998 and references therein).

- (c) The discrepancy between the chemical abundances derived from forbidden and permitted emission-lines (Kaler 1986; Peimbert, Storey & Torres-Peimbert 1993), which could be explained by the presence of condensations (Viegas & Clegg 1994; Liu et al. 2000).

Regarding active galactic nuclei, self-consistent models reproducing both the emission-line and continuum spectra of selected objects indicate that shocks are present in the narrow-line region (Contini, Prieto & Viegas 1998a,b; Contini & Viegas 1999).

In the following, the main issues associated with photoionization models are reviewed. In particular, models for the well-known H II galaxy, I Zw 18, are discussed, and possible explanations for the discrepancy between model results and observational data are suggested.

2. STAR FORMING GALAXIES

Due to its low metallicity, I Zw 18 is one of the extragalactic H II regions used to derive the primordial He abundance. Recently, Stasińska & Schaerer (1999, hereinafter SS99) presented 1-D models for the NW knot of I Zw 18. They concluded that in addition to photoionization, another heating mechanism is necessary to explain all observed features. On the other hand, in starburst galaxies, shocks must be contributing to the observed emission-lines depending on the evolutionary phase of the stellar cluster (Viegas, Contini & Contini 2000). Could this be the case for I Zw 18? In order to answer this question, photoionization models for I Zw 18 are re-examined.

2.1. *I Zw 18: the SS99 model*

A 1-D spherically symmetric photoionization model for the NW knot of I Zw 18 was proposed by SS99, assuming the ionizing radiation spectrum of a stellar cluster, a density of 100 cm^{-3} (as indicated by the [S II] line ratio) and chemical abundances derived by Izotov & Thuan (1998). In defining the best fit, the criteria adopted were that the relevant emission-line ratios must be reproduced, as well as the size of the ionized region and its luminosity.

Adjusting the total initial mass of the stellar cluster in order to reproduce the luminosity, the authors show that a homogeneous model may explain some of the line ratios, but the calculated size of the ionized region is too small unless a filling factor of the

order of 10^{-2} is adopted. Notice that the HST image of I Zw 18 (see Figure 1 of SS99) shows an inhomogeneous gas distribution which could justify models with a filling factor less than unity. The homogeneous model with $\epsilon = 10^{-2}$ combined with condensations provided the best-fit. All the criteria were fulfilled except for the [O III] $\lambda 4363/5007$ line ratio, which was too low compared to observations. Since this line ratio is a known temperature indicator, the authors concluded that an additional heating mechanism must be present in the NW knot of I Zw 18.

2.2. *Shocks in Star Forming Regions*

The detection of the infrared line [O IV] $25.9 \mu\text{m}$, in addition to [Ne II] $12.8 \mu\text{m}$ and [Ne III] $15.6 \mu\text{m}$ in a number of well-known starburst galaxies has been reported by Lutz et al. (1998). Using simple photoionization models, these authors showed that photoionization by a stellar cluster was not enough to explain the presence of the highly ionized species. They suggested other possible mechanisms that could contribute to the emission-lines. They concluded that shocks related to stellar activity must prevail in these objects. However, it was shown that the presence of hot Wolf-Rayet stars could explain the observed [O IV] emission for two galaxies of the Lutz sample: NGC 5253 and II Zw 40 (Schaerer & Stasińska 1999). But even considering WR stars, photoionization models are unable to explain the observations of the other sample galaxies, leading Schaerer & Stasińska to conclude that an alternative mechanism is required.

To analyse the galaxies of the Lutz sample, Viegas, Contini, & Contini (1999) used composite models, coupling the effect of photoionization by a stellar cluster and shocks.

The numerical simulations were performed using the SUMA code (see, for instance, Viegas & Contini 1997). This code has been used since the 1980's to study the narrow-line regions of active galactic nuclei. The ionization and heating equations are solved for a plane-parallel cloud, taking into account the coupled effect of ionizing radiation and shocks, and also accounting for the diffuse radiation produced by the hot gas. Due to this self-consistency, SUMA models are more realistic than those obtained by the so-called ionizing shock models, which only account for the diffuse radiation generated by the hot gas. However it is well known that a radiation source is always present in AGN, planetary nebulae and H II regions, and although its effect on the physical conditions of the gas may be less important than shocks, it is hardly negligible and cannot be turned off.

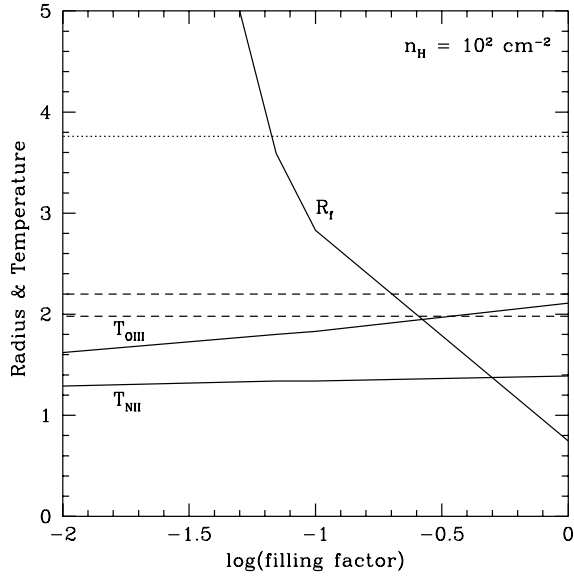


Fig. 1. The size of the ionized gas ($R_f/10^{19}$) and the gas temperature ($T/10^4$ K) as a function of the filling factor adopted in the photoionization model. The dotted line indicates the observed value of the radius, whereas the dashed lines indicate the range associated with the gas temperature deduced from the [O III] line ratios. Although observations are not available for the [N II] line ratio, the corresponding temperature obtained from the models is also plotted.

There are two types of composite models depending on the location of the cloud relative to the radiation source and the shock front. In one case, both ionizing mechanisms affect the same edge of the cloud, whereas in the other case, they act on opposite edges. In the latter case, the effects of photoionization and shocks may overlap through the diffuse radiation, provided the cloud is not too wide. Regarding the simulations, in addition to the input parameters usually used in photoionization models (ionizing radiation spectrum, density distribution and chemical abundances), the composite models requires the shock velocity, the pre-shock density and the geometrical thickness of the cloud.

Assuming a black-body spectrum, and a range of shock velocities and pre-shock densities, single-cloud models have been built for the starburst galaxies of Lutz sample. The results are compared to the observed infrared line ratios using a diagnostic diagram $[\text{O IV}]/([\text{Ne II}] + 0.44[\text{Ne III}])$ versus $[\text{Ne III}]/[\text{Ne II}]$, as suggested by Lutz et al. (1998). In the diagram, the data points are distributed along a diagonal, going from the bottom-left corner to the top-right corner. The points corresponding to the two galaxies

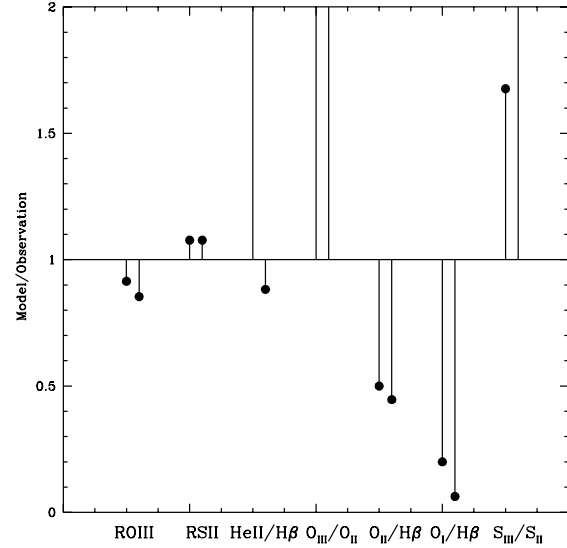


Fig. 2. Comparing observational and theoretical intensity ratios of the relevant emission-lines:

$$R_{\text{OIII}} = [\text{O III}] 4363/5007, R_{\text{SII}} = [\text{S II}] 6717/6731, \\ \text{He II } 4686/\text{H}\beta, \quad ([\text{O III}] 5007 + 4959)/[\text{O II}] 3727, \\ [\text{O II}] 3727/\text{H}\beta, \quad ([\text{O I}] 6300 + 6363)/\text{H}\beta, \quad \text{and} \\ [\text{S III}] 6312/([\text{S II}] 6727 + 6731).$$

The results correspond to a uniform density cloud (30 cm^{-3}), photoionized by a stellar cluster. For each line ratio, the symbols on the left correspond to a 3.3 Myr stellar cluster, while those on the right to a 5.4 Myr stellar cluster.

NGC 5253 and II Zw 40, studied by Schaerer & Stasińska (1999), are located at the top/right zone.

Assuming that all the objects are photoionized by a similar radiation spectrum, our single-cloud results show that the distribution on the diagram can be reproduced if the shock velocity and the pre-shock density increase from the top to the bottom part of the diagonal. When the intensity of ionizing radiation is kept constant, the higher the shock velocity the stronger is the shock effect on the physical conditions in the cloud, relative to photoionization. Since NGC 5253 and II Zw 40 data points are located in the low-velocity/low-density zone, photoionization is expected to be the dominant mechanism for these two objects, while shocks are required for explaining the data for the other objects, in agreement with Lutz et al. (1998).

From our results, the observed trend can be interpreted as a sequence between two extreme cases: starburst regions, where high velocity shocks are present and give a significant contribution to gas ionization, and radiation-dominated objects (H II galax-

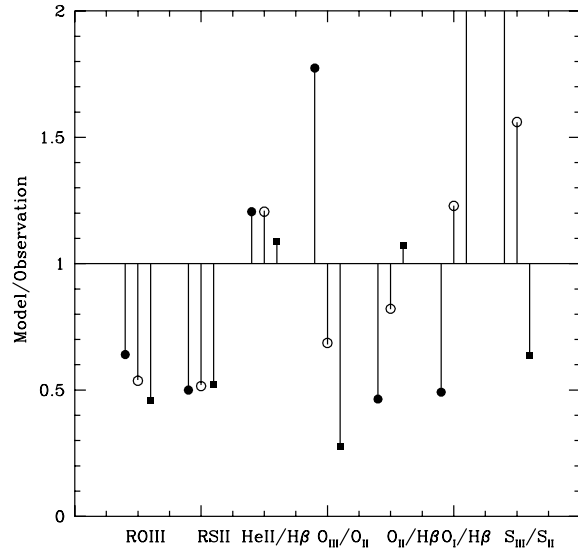


Fig. 3. Same as Fig. 2, but for a high-density filament (10^4 cm^{-3}) photoionized by a 5.4 Myr stellar cluster. For each line ratio, three results are shown corresponding to different locations of the filament in the H II region: at the nebula inner edge (solid dots), and at distances from the stellar cluster where 25% (solid squares) and 75% (circles) of H β has already been emitted.

ies), where photoionization is the dominant mechanism. As showed by Viegas et al. (1999), the distinction between these two kinds of galaxies can be understood in terms of temporal evolution. In H II galaxies, like NGC 5253 and II Zw 40, the star forming region is young enough to contain a high fraction of massive O and WR stars which produce a large amount of ionizing photons. On the other hand, in starburst galaxies such as M 82 and NGC 253, the star formation event is much older and the massive stars have already evolved to a SN phase. As the stellar cluster evolves, the ratio between the mechanical energy from the SNe and the ionizing Lyman continuum rapidly increases (Leitherer & Heckman 1995). Thus, radiation-dominated H II galaxies must be associated with young metal poor objects, whereas starburst galaxies with massive evolved objects.

Since I Zw 18 has the characteristics of an H II galaxy, we expect photoionization to be the major ionizing mechanism. Thus, in the following we review the photoionization model presented by SS99, which indicated the need for an additional heating mechanism.

3. REVIEWING THE NW KNOT OF I ZW 18

The suggestion of an additional ionizing mechanism in the NW knot of I Zw 18 came from the fact that the photoionization models proposed by Stasińska & Schaerer (1999) were unable to reproduce the [O III] line ratio. This line ratio is a temperature indicator, and their models gave an average gas temperature too low compared to that derived from the observations.

To analyze the problem, the model assumptions are reviewed and a new model is proposed using the 1-D photoionization code Aangaba (Gruenwald & Viegas 1992). In the following, the initial models are built assuming the same input parameters adopted by SS99, i.e., $n_{\text{H}} = 100 \text{ cm}^{-3}$, a stellar cluster ionizing continuum and the Izotov & Thuan (1998) chemical abundances.

The results shown in Figure 1 correspond to a spherically symmetric nebula photoionized by a continuum due to a 3.3 Myr old stellar cluster (Cid-Fernandes et al. 1992). The total mass is chosen in order to reproduce the observed luminosity. It is easily verified that, unless the filling factor is of order 10^{-2} , the size of the ionized region is too small.

On the other hand, as ϵ approaches unity, the gas temperature defined by the [O III] ratio becomes higher. Notice that photoionization models can match the observed gas temperature $T_{\text{O III}}$ as long as the adopted filling factor is higher than 0.3. In this case, however, the calculated outer radius is far below the observed value.

The net effect of 1-D models with ϵ lower than unity is to provide a slower increase of the optical depth with the distance from the central source (see, for instance, Osterbrock 1989). This leads to an increase of the size of the low-ionization zone with respect to the high-ionization zone, which results in lower average temperatures derived from more ionized species, as in the case of the [O III] lines.

A possible way to increase the ionized zone without decreasing the average gas temperature is to assume $\epsilon = 1$ and a gas density lower than 100 cm^{-3} . This value was adopted by SS99 in order to reproduce the observed [S II] line ratio from Izotov & Thuan (1998). However, it is well-known that the [S II] line ratio is practically constant for densities lower than a few hundred. Therefore, models with a density of the order of 30 cm^{-3} and $\epsilon = 1$ can reproduce both the size of the ionized region and the $T_{\text{O III}}$ temperature. The emission-line ratios relevant to constrain this model are shown in Figure 2, where observed values are compared to the values coming from a uniform gas distribution with density equal

to 30 cm^{-3} , $\epsilon = 1$, and assuming ionization from stellar clusters of two different ages: 3.3 Myr and 5.4 Myr. The latter gives a better fit for $\text{He II}/\text{H}\beta$. On the other hand, $[\text{O III}]/[\text{O II}]$ and $[\text{S III}]/[\text{S II}]$ are too high, while $[\text{O II}]/\text{H}\beta$ and $[\text{O I}]/\text{H}\beta$ are too low.

The same kind of discrepancy between observational and theoretical line ratios was reported by SS99 concerning the homogeneous model. These authors suggested the presence of condensations to avoid the fitting problems. In Figure 3, results are shown for filaments with density equal to 10^4 cm^{-3} , located at different distances from a stellar cluster. Notice that the results can be very different. A real model for the NW knot of I Zw 18 should account for the contributions of the diluted gas as well as of the different filaments. It is clear that a model can be obtained with the same degree of accuracy as obtained by SS99 but with the additional advantage of also fitting the $[\text{O III}]$ line ratio.

However, more than finding the best model for I Zw 18, the goal here is to illustrate how assumptions used to build a model that satisfies practically all the observational constraints, could still lead to a wrong conclusion. Indeed, models with a filling factor lower than unity and higher density (100 cm^{-3}) indicated that an additional energy source was required, while models with $\epsilon = 1$ and lower density (30 cm^{-3}) offer a fitting of the line ratios, $\text{H}\beta$ luminosity and size of the ionized region without that requirement. Thus, pure photoionization can explain I Zw 18 observations, as expected from the analysis of the infrared lines of star forming objects (Viegas et al. 1999).

4. CONCLUDING REMARKS

The improvement of spatial resolution, revealing more and more details of the emitting regions of different classes of objects, showing the presence of clumps and voids, as well as the improvement in signal/noise, providing more accurate line intensities, require a more realistic approach.

It seems clear to me that if 1-D models are used to analyze the emission-line spectra of clumpy objects, the use of a filling factor less than unity should be avoided. As shown in the case of the NW knot of I Zw 18, in this kind of model the conclusions may be misleading because the effect of $\epsilon < 1$ is to artificially increase the low-ionization zone of the cloud. As a consequence, optically thick models will artificially decrease the average temperature of the high-ionization zone (see Fig. 1) and artificially increase the intensity of the low ionization lines. Thus, the chance of reaching a wrong conclusion about the gas temperature or the ionic fraction low-ionization

species is very high. In the first case, the presence of additional heating source required by the model may not be necessary, as illustrated by the discussion of I Zw 18. In the second case, mimicking a higher ionic fraction for the low-ionization species may reflect both on the elemental abundances deduced from the model, as well as on the choice of the other input parameters. A good example is the model used by Alexander et al. (1999) to study the ionizing continuum of NGC 4151. Their best-fit model for the infrared lines corresponds to a filling factor $\epsilon < 1$. Based on this model they discard the existence of a big blue bump just beyond the Lyman limit because “*such a bump clearly overproduces the low-ionization lines and underproduces the high-ionization lines*”. Notice however that this could also be a consequence of the filling factor adopted by the authors.

A better and safer way to study clumpy regions with 1-D models was proposed more than a decade ago by Viegas-Aldrovandi & Gruenwald (1988) when studying the narrow-line regions of AGN. Several models with different physical conditions are combined to produce the observed emission-line spectra. This method has also been used by Contini et al. (1998a,b; Contini & Viegas 1999) to reproduce the emission-line and continuum spectra of Circinus, NGC 5252 and NGC 4051 self-consistently.

Certainly a better approach to emission-line objects is to use a 3-D photoionization model, specially if imaging and spectroscopic data with high spatial resolution are available (Morisset et al. 2000). A good example is the planetary nebula NGC 3132. Its imaging seems to indicate that it has ellipsoidal geometry. However, using a 3D code, Monteiro et al. (2000, 2001) showed that a model with an ellipsoidal geometry could not reproduce all the observational data. In fact, only a hourglass (diabolo) shape could provide a self-consistent fit to the image, the emission-line spectrum, the electron density distribution and the velocity field. There is no doubt that 3-D models will become the tools of choice analyzing emission-line objects.

Based on all the discussion above, let me end with a warning: *When dealing with models, beware of possible illusions...*

I am very grateful to my friends Ruth Gruenwald, Marcella Contini and M. Almudena Prieto for a long and fruitful collaboration, which permitted me to present this paper. I am also indebted to Gary Steigman for a careful proofreading. This work has been partially supported by PRONEX/Finep (41.96.0908.00) and CNPq (304077/77.1)

REFERENCES

- Alexander, T., Sturm, E., Lutz, D., Sternberg, A., Netzer, H., & Genzel, R. 1999, *ApJ*, 512, 204.
- Cid-Fernandes, R., Dottori, H., Gruenwald, R., & Viegas, S. M. 1992, *MNRAS*, 255, 165
- Contini, M., Prieto, M. A., & Viegas, S. M. 1998a, *ApJ*, 492, 511
- Contini, M., Prieto, M. A., & Viegas, S. M. 1998b, *ApJ*, 505, 621
- Contini, M. & Viegas, S. M. 1999, *ApJ*, 523, 114
- Ferland, G. J., et al. 1995, in *The Analysis of Emission Lines*, eds. R. E. Williams & M. Livio (Cambridge: CUP), 83
- Ferland, G. J. 2000, *RevMexAA(SC)*, 9, 153
- Gruenwald, R., & Viegas, S. M. 1992, *ApJS*, 78, 153
- Gruenwald, R., Viegas, S. M. & Broguière, D. 1997, *ApJ*, 480, 283
- Izotov, Y. I., & Thuan, T. X. 1998, *ApJ*, 497, 227
- Kaler, J. B. 1986, *ApJ*, 308, 337
- Leitherer, C., & Heckman, T. H. 1995, *ApJS*, 96, 9
- Liu, X., & Danziger, J. 1993, *MNRAS*, 263, 256
- Liu, X. et al. 2000, *MNRAS*, 312, 585
- Lutz, D., Kunze, D., Spoon, H. W. W., & Thornley, M. D. 1998, *A&A*, 333, L75
- Mathis, J. S., Torres-Peimbert, S., & Peimbert, M. 1998, *ApJ*, 495, 328
- Monteiro, H., Morisset, C., Gruenwald, R., & Viegas, S. M. 2000, *ApJ*, 537, 853
- Monteiro, H., Gruenwald, R. & Morisset, C. 2002, *RevMexAA(SC)*, 12, 170 (this volume)
- Morisset, C., Gruenwald, R., & Viegas, S. M. 2000, *ApJ*, 533, 931
- Och, S. R., Lucy, L. B., & Rosa, M. R. 1998, *A&A*, 336, 301
- Osterbrock, D. E. 1989, In: *Astrophysics of Gaseous Nebulae and Active Galactic Nuclei*, University Science Books (Mill Valley, California: USB)
- Osterbrock, D. E., & Flatter, E. 1959, *ApJ*, 129, 26
- Peimbert, M., & Costero, R. 1969, *Bol. Obs. Tonantzintla y Tacubaya*, 5, 3
- Peimbert, M., Storey, M. J., & Torres-Peimbert, S. 1993, *ApJ*, 414, 626
- Schaerer, D., & Stasińska, G. 1999, *A&A*, 345, L17
- Stasińska, G., & Schaerer, D. 1999, *A&A*, 351, 72
- Viegas, S. M., & Clegg, R. E. 1994, *MNRAS*, 271, 993
- Viegas-Aldrovandi, S. M., & Gruenwald, R. 1988, *ApJ*, 324, 683
- Viegas, S. M., & Contini, M. 1997, in *IAU Colloquium 159, ASP Conf. Ser. 113, Emission Lines in Active Galaxies: New Methods and Techniques*, eds. B. Peterson & A. Wilson (San Francisco: ASP), 365
- Viegas, S. M., Contini, M. & Contini, T. 1999, *A&A*, 347, 112